IFT-UAM/CSIC-22-134

Machine-Learned Exclusion Limits without Binning

Ernesto Arganda [a,b*] **Andres D. Perez,** [b†] **Martin de los Rios** [a,c‡] **and Rosa María Sandá Seoane** [a§]

[a] *Instituto de Física Teórica UAM-CSIC, C/ Nicolás Cabrera 13-15, Campus de Cantoblanco, 28049, Madrid, Spain*

[b] *IFLP, CONICET - Dpto. de Física, Universidad Nacional de La Plata, C.C. 67, 1900 La Plata, Argentina*

[c] *Departamento de Física Teórica, Universidad Autónoma de Madrid, E-28049 Cantoblanco, Madrid, Spain*

arXiv:2211.04806v1 [hep-ph] 9 Nov 2022

Abstract

Machine-Learned Likelihoods (MLL) is a method that, by combining modern machine-learning classification techniques with likelihood-based inference tests, allows to estimate the experimental sensitivity of high-dimensional data sets. We extend the MLL method by including the exclusion hypothesis tests and show that the addition of Kernel Density Estimators avoids the need to bin the classifier output in order to extract the resulting one-dimensional signal and background probability density functions. We first test our method on toy models generated with multivariate Gaussian distributions, where the true probability distribution functions are known. We then apply it to a case of interest in the search for new physics at the HL-LHC, in which a Z' boson decays into lepton pairs, comparing the performance of our method for estimating 95% CL exclusion limits to the results obtained applying a binned likelihood to the machine-learning classifier output.

* ernesto.arganda@csic.es
† andres.perez@iflp.unlp.edu.ar
‡ martin.delosrios@uam.es
§ r.sanda@csic.es

Contents

1 Introduction 1

2 Method 2

3 Application examples 5

3.1 Known true PDFs: multivariate Gaussian distributions 5

3.2 SSM Z' boson decaying into lepton pairs at the LHC 7

4 Conclusions 8

1 Introduction

Modern machine learning (ML) has become a fundamental tool in experimental and phenomenological analyses of high-energy physics (for reviews see, for instance, [1–9] and for pioneer papers see [10–12]). The ML algorithms can be applied not only to event-by-event collider analyses, but also used at the event-ensemble level [13–20]. In order to estimate the experimental sensitivity to potential new-physics signals at colliders, several studies have recently appeared that combine the use of ML classifiers with traditional statistical tests [21–36]. More specifically, it was shown in [21] that the calibration of classifiers trained to distinguish signal and background samples under the relevant hypotheses ensures to properly estimate the likelihood ratio and consequently can be used to compute a statistical significance. Recently, a simplification of [21] has been proposed in [36], the so-called Machine-Learned Likelihoods (MLL), which computes the expected experimental sensitivity through the use of ML classifiers, utilizing the entire discriminant output. A single ML classifier estimates the individual probability densities and subsequently one can calculate the statistical significance for a given number of signal and background events (S and B, respectively) with traditional hypothesis tests. By construction, the output of the classifier is always one-dimensional, so we reduce the hypothesis test to a single parameter of interest, the signal strength μ. On the one hand, it is simply and reliably applicable to any high-dimensional problem. On the other hand, using all the information available from the ML classifier does not require defining working points like traditional cut-based analyses. The ATLAS and CMS Collaborations incorporate similar methods in their experimental analyses, but consider only the classifier output as a good variable to bin and fit the binned likelihood formula (see, for instance, Refs. [37–44]).

The MLL code [45] developed in [36] only includes the calculation of the discovery hypothesis test, although the expressions needed to calculate the exclusion limits were provided. In [46] we extend the MLL method by adding the exclusion hypothesis test. In this paper, we improve the MLL method with the use of Kernel Density Estimators (KDE) [47, 48], in order to avoid to bin the ML classifier output for extracting the resulting one-dimensional signal

and background probability density functions, as proposed in [36, 46].

The structure of the paper is the following: Section 2 is devoted to summarizing the main features of the MLL method with the relevant expressions for the calculation of exclusion limits and the implementation of KDE in it. In Section 3 we show the performance of the MLL method with KDE in two different application examples: in Section 3.1 a case where the true probability density functions (PDFs) are known, through a toy model generated with multivariate Gaussian distributions; and in Section 3.2, we present an HL-LHC study for Sequential Standard Model (SSM) [49] Z' bosons decaying into lepton pairs, comparing the MLL+KDE performance for estimating 95% CL exclusion limits with the results obtained applying a binned likelihood to the machine learning classifier output and also with respect to the projections reported by the ATLAS Collaboration for an LHC center-of-mass energy of $\sqrt{s} = 14$ TeV with a total integrated luminosity of $\mathcal{L} = 3$ ab^{-1} [50]. Finally, Section 4 summarizes our more important results and conclusions.

2 Method

In this section, we present the corresponding formulae for the estimation of exclusion sensitivities with the MLL method, first introduce in [36, 46]. We summarize the main features of the method which allows dealing with data of arbitrarily high dimension through a simple ML classifier while using the traditional inference tests to compare a null hypothesis (the signal-plus-background one) against an alternative one (the background-only one). We also present the details of the implementation of KDE to obtain the unbinned posterior probability distributions from the classifier output, needed to compute the corresponding likelihood functions.

Following the statistical model in [51], we can define the likelihood $\mathcal{L}$ of N independent measurements with an arbitrarily high-dimensional set of observables x as

$$\mathcal{L}(\mu, s, b) = \mathrm{Poiss}\big(N|\mu S + B\big) \prod_{i=1}^{N} p(x_i|\mu, s, b)\,, \tag{1}$$

where S (B) is the expected total signal (background) yield, Poiss stands for a Poisson probability mass function, and $p(x|\mu, s, b)$ is the probability density for a single measurement x, where μ defines the hypothesis we are testing for.

We can model the probability density containing the event-by-event information as a mixture of signal and background densities

$$p(x|\mu, s, b) = \frac{B}{\mu S + B}\, p_b(x) + \frac{\mu S}{\mu S + B}\, p_s(x)\,, \tag{2}$$

where $p_s(x) = p(x|s)$ and $p_b(x) = p(x|b)$ are, respectively, the signal and background probability densities for a single measurement x, and $\frac{\mu S}{\mu S+B}$ and $\frac{B}{\mu S+B}$ are the probabilities of an event being sampled from the corresponding probability distributions.

To derive upper limits on μ, and in particular considering additive new physics scenarios ($\mu \geq 0$), we need to consider the following test statistic for exclusion limits [52]:

$$\tilde{q}_\mu = \begin{cases} 0 & \text{if } \hat{\mu} > \mu\,, \\ -2\ \mathrm{Ln}\ \frac{\mathcal{L}(\mu,s,b)}{\mathcal{L}(\hat{\mu},s,b)} & \text{if } 0 \leq \hat{\mu} \leq \mu\,, \\ -2\ \mathrm{Ln}\ \frac{\mathcal{L}(\mu,s,b)}{\mathcal{L}(0,s,b)} & \text{if } \hat{\mu} < 0\,, \end{cases} \tag{3}$$

where $\hat{\mu}$ is the parameter that maximizes the likelihood in Eq. (1)

$$\sum_{i=1}^{N} \frac{p_s(x_i)}{\hat{\mu} S\, p_s(x_i) + B\, p_b(x_i)} = 1\,. \tag{4}$$

Considering our choice for the statistical model in Eq. (1), $\tilde{q}_\mu$ turns out

$$\tilde{q}_\mu = \begin{cases} 0 & \text{if } \hat{\mu} > \mu \\ 2(\mu - \hat{\mu})S - 2\sum_{i=1}^{N}\ \mathrm{Ln}\ \left(\frac{Bp_b(x_i)+\mu S p_s(x_i)}{Bp_b(x_i)+\hat{\mu} S p_s(x_i)}\right) & \text{if } 0 \leq \hat{\mu} \leq \mu \\ 2\mu S - 2\sum_{i=1}^{N}\ \mathrm{Ln}\ \left(1 + \frac{\mu S p_s(x_i)}{Bp_b(x_i)}\right) & \text{if } \hat{\mu} < 0; \end{cases} \tag{5}$$

Since $p_{s,b}(x)$ are typically not known, the base idea of our method in [36] is to replace these densities for the one-dimensional manifolds that can be obtained for signal and background from a machine-learning classifier. After training the classifier with a large and balanced dataset of signal and background events, it can be obtained the classification score $o(x)$ that maximizes the binary cross-entropy (BCE) and thus approaches [21, 53]

$$o(x) = \frac{p_s(x)}{p_s(x) + p_b(x)}\,, \tag{6}$$

as the classifier approaches its optimal performance. The dimensionality reduction can be done by dealing with $o(x)$ instead of x, using

$$p_s(x) \to \tilde{p}_s(o(x))\,, \qquad \text{and} \qquad p_b(x) \to \tilde{p}_b(o(x))\,, \tag{7}$$

where $\tilde{p}_{s,b}(o(x))$ are the distributions of $o(x)$ for signal and background, obtained by evaluating the classifier on a set of pure signal or background events, respectively. Notice that this allows us to approximate both signal and background distributions individually, retaining the full information contained in both densities, without introducing any working point. These distributions are one-dimensional, and therefore can always be easily handled and incorporated into the test statistic in Eq. (5)

$$\tilde{q}_\mu = \begin{cases} 0 & \text{if } \hat{\mu} > \mu \\ 2(\mu - \hat{\mu})S - 2\sum_{i=1}^{N}\ \mathrm{Ln}\ \left(\frac{B\tilde{p}_b(o(x_i))+\mu S\tilde{p}_s(o(x_i))}{B\tilde{p}_b(o(x_i))+\hat{\mu} S\tilde{p}_s(o(x_i))}\right) & \text{if } 0 \leq \hat{\mu} \leq \mu \\ 2\mu S - 2\sum_{i=1}^{N}\ \mathrm{Ln}\ \left(1 + \frac{\mu S\tilde{p}_s(o(x_i))}{B\tilde{p}_b(o(x_i))}\right) & \text{if } \hat{\mu} < 0; \end{cases} \tag{8}$$

as well as into the condition on $\hat{\mu}$ from Eq. (4)

$$\sum_{i=1}^{N} \frac{\tilde{p}_s(o(x_i))}{\hat{\mu} S\, \tilde{p}_s(o(x_i)) + B\, \tilde{p}_b(o(x_i))} = 1\,. \tag{9}$$

The test statistic in Eq. (8) is estimated through a finite dataset of N events and thus has a probability distribution conditioned on the true unknown signal strength μ'. For a given hypothesis described by the μ' value, we can estimate numerically the $\tilde{q}_\mu$ distribution. When the true hypothesis is assumed to be the background-only one ($\mu' = 0$), the median expected exclusion significance med $[Z_\mu|0]$ is defined as

$$\text{med}\ [Z_\mu|0] = \sqrt{\text{med}\ [\tilde{q}_\mu|0]}\,, \tag{10}$$

where we estimate the $\tilde{q}_\mu$ distribution by generating a set of datasets with background-only events. Then, to set upper limits to a certain confidence level, we select the lowest μ which achieves the required median expected significance.

It is worth remarking that the output of the machine learning classifier, for a given set of events, gives us a sample of the desired PDFs $\tilde{p}_{s,b}(o(x))$. Hence, to apply Eq. (8) we first need to extract the classifier posteriors. As these samples are one-dimensional, we can always compute binned PDFs, as was done in [36]. Binning the output variable is a typical procedure when using ML tools. Nevertheless, it is also possible to compute the PDFs through other parametric (such as Mixture Models [54]) or non-parametric methods (such as Kernel Density Estimation (KDE) [47, 48] or Neural Density Estimation [55]). In this work, we made extensive use of the KDE method[1], through its `scikit-learn` implementation [57].

Given a set of N events that were previously classified by the machine learning as signal (background) events, the PDF estimated by the KDE method is defined as

$$p_{s,b}(o(x)) = \frac{1}{N} \sum_{i}^{N} \kappa_\epsilon \left[o(x) - o(x_i)\right] \tag{11}$$

where κ_ϵ is a kernel function that depends on the "smoothing" scale, or bandwidth parameter ϵ. There are several different options for the kernel function. In this work, we used the *Epanechnikov kernel* [58] as it is known to be the most efficient kernel [55]. This kernel is defined as

$$\kappa_\epsilon(u) = \begin{cases} \frac{1}{\epsilon}\frac{3}{4}\left(1 - (u/\epsilon)^2\right), & \text{if } |u| \leq \epsilon \\ 0, & \text{otherwise} \end{cases}$$

[1]During the completion of this work, Ref. [56] has appeared, in which data-driven methods are used for dealing with unbinned multivariate EFT observables. Although this work is similar to ours in the spirit of avoiding the binning of multidimensional variables, there are significant differences in the application of ML and KDE algorithms between our MLL+KDE method and the ML4EFT framework of [56].

It is important to remark that the "bandwidth" parameter ϵ censors the degree of smoothness. Hence, a very low ϵ will overfit the data, whereas a very high ϵ will underfit it. Also is worth remarking that although KDEs method suffers from the curse of dimensionality, we are applying such technique to the one-dimensional output of the machine learning classifier avoiding this problem.

For completeness, we also introduce here the median exclusion significance estimation for the traditional Binned Likelihood (BL) method and the use of Asimov datasets [52], which will be used to compare our technique

$$\text{med}[Z_\mu|0] = \sqrt{\tilde{q}_\mu} = \left[2\sum_{d=1}^{D}\left(B_d \text{ Ln } \left(\frac{B_d}{S_d+B_d}\right) + S_d\right)\right]^{1/2}, \tag{12}$$

where S_d and B_d are the expected number of signal and background events in each bin d. This approximation is very effective but runs into trouble when the dimension of the data grows, which is known as the curse of dimensionality since the number of data points required to reliably populate the bins scales exponentially with the dimension of the observables x. This is a non-existent problem in our method, which always reduces the original dimension to one as stated in Eq. (7), allowing the application of the BL method to the classifier output, as also done by experimental collaborations when using ML methods, as mentioned in Section 1.

3 Application examples

3.1 Known true PDFs: multivariate Gaussian distributions

To show the performance of the MLL method with KDE we first analyze toy models generated with multivariate Gaussian distributions $\mathcal{N}_{dim}(\boldsymbol{m}, \boldsymbol{\Sigma})$ of different dimensions. For simplicity, in these examples, we set no correlation between the abstract variables (i.e., covariance matrices $\boldsymbol{\Sigma} = \mathbb{I}_{dim\times dim}$).

We start with the simplest case, consisting of an abstract two-dimensional space (x_1, x_2). Events are generated by Gaussian distributions $\mathcal{N}_2(\boldsymbol{m}, \boldsymbol{\Sigma})$, with $\boldsymbol{m} = +0.3(-0.3)$ for S (B). We trained a supervised per-event classifier, `XGBoost`, with 1M events per class (balanced dataset), to distinguish S from B. The classifier output, $o(x)$, can be found in the left panel of Figure 1, for two new independent datasets of pure signal (blue) and pure background (red) events. We present the estimations of $\tilde{p}_{s,b}(o(x))$ using two methods: binning $o(x)$ (shaded regions), and KDE with Epanechnikov kernel (dashed curves). For the latter, the tuning of the bandwidth was done empirically via a cross-validated grid-search over a parameter grid with the `GridSearchCV` algorithm, from the `scikit-learn` python library. As already mentioned, the choice of a bandwidth value is a key feature of any KDE implementation to properly fit the data. For the different examples shown in this manuscript, we used the grid-search approach with good results, although computationally expensive. For other examples,

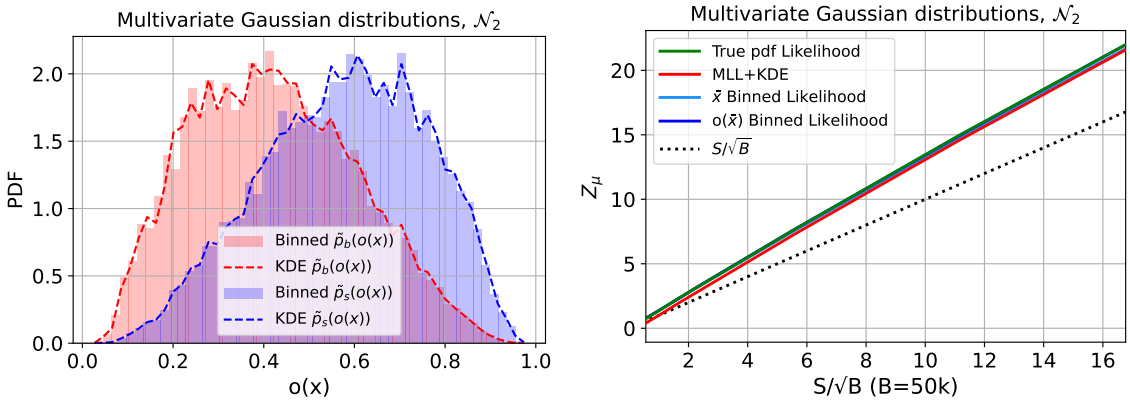

Figure 1: Results for the $\mathcal{N}_2(\boldsymbol{m}, \boldsymbol{\Sigma})$ case. *Left Panel:* Output of the `XGBoost` classifier. *Right Panel:* Exclusion significance for the different methods, for fixed $\langle B \rangle = 50$k, and different signal strengths $\langle S \rangle$. The green line shows the results obtained using the true PDFs, while the red line shows the results implementing the MLL+KDE method. Dark and light blue lines represent the result of applying the BL method to the classifier output and the original variables respectively. Finally, the black dotted line represents the usual counting method, $S/\sqrt{B}$.

a different method to estimate the bandwidth may be needed, however, a deeper exploration of this technical issue is out of the scope of this work.

In the right panel of Figure 1 we show the results for the MLL exclusion significance with KDE considering an example with a fixed background of $\langle B \rangle = 50$k and different signal strengths. We also include the significance calculated using the true probability density functions in Eq. (3), and the results employing a binned Poisson log-likelihood of the original two-dimensional space (x_1, x_2) with Eq. (12), which is possible to compute in this simple scenario. For completeness, we also include the results binning the one-dimensional ML output variable for obtaining the PDFs as in [36, 46]. As can be seen, since we are analyzing a simple example, the significances estimated with all the methods are indistinguishable from the ones estimated with the true PDFs, which is expected given the low dimensionality of the space.

The advantage of the MLL+KDE method against traditional approaches appears when dealing with $dim = n$, with $n > 2$. In Figure 2 we present the exclusion significance for higher dimensional data generated with $\mathcal{N}_n(\boldsymbol{m}, \boldsymbol{\Sigma})$, $\boldsymbol{\Sigma} = \mathbb{I}_{n\times n}$, and $\boldsymbol{m} = +0.3(-0.3)$ (left panel) and $\boldsymbol{m} = +0.7(-0.7)$ (right panel) for S (B). It is worth reminding that the Binned-Poisson Likelihood method becomes intractable in the original high-dimensional space. On the other hand, the results with the MLL+KDE method approach the ones with the true generative functions in both cases ($\boldsymbol{m} = \pm 0.3$ and $\boldsymbol{m} = \pm 0.7$) for all the analyzed dimensions. It is important to highlight that the ML output is always one-dimensional regardless of the dimension of the input data and, hence, can always be easily binned. For completeness, we

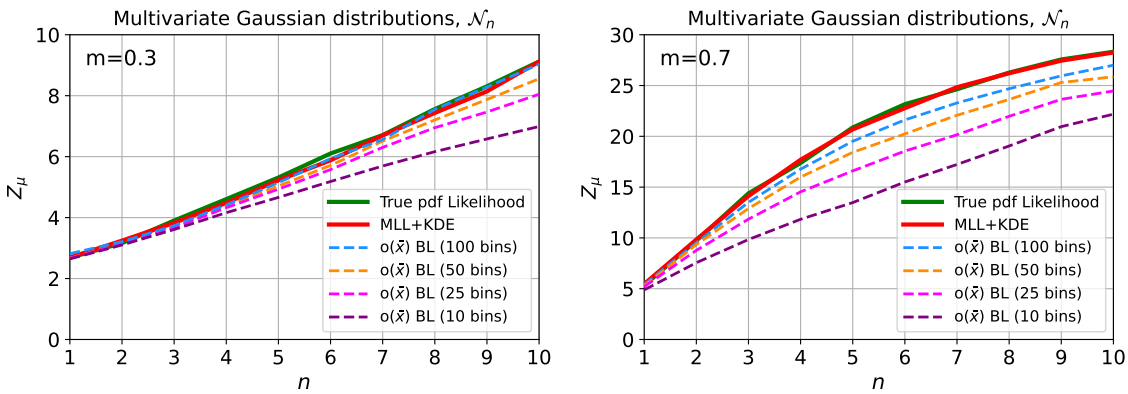

Figure 2: Exclusion-limit significance for $\mathcal{N}_{dim}(\boldsymbol{m}, \boldsymbol{\Sigma})$, as a function of the dim, for fixed $\langle B \rangle = 50\text{k}$ and $\langle S \rangle = 500$. The red solid curve shows the result of implementing the MLL+KDE method, while the green curve shows the results obtained using the true PDFs. Dashed color curves represent the results obtained by applying the BL method to the classifier one-dimensional output for different bin numbers. *Left panel:* $\boldsymbol{m} = +0.3(-0.3)$ for S (B). *Right panel:* $\boldsymbol{m} = +0.7(-0.7)$ for S (B).

show in Figure 2 the significances obtained by applying a BL method to the machine learning output with different bin numbers. As can be seen, when increasing the bin number the result approaches the ones obtained with the MLL+KDE method and with the true PDFs.

Although these are toy models they allow us to understand the performance of MLL with KDE method over problems of different complexity and demonstrate its improvement with respect to the BL method applied to the classifier output. Particularly the MLL+KDE has a stable behavior when increasing the dimensionality of the input space, as well as when increasing the separation of the signal and background distributions on the original abstract variables. On the other hand, the BL method applied to the classifier output departs from the results obtained with the true PDFs as the number of dimensions and separation of signal and background samples increases. The number of bins to use is another limitation, non-existent in our method that uses a non-parametric technique for PDF extraction.

3.2 SSM Z' boson decaying into lepton pairs at the HL-LHC

In this section, we analyzed the performance of our method on a simple collider example, namely the search of an SSM Z' boson decaying into lepton pairs at the HL-LHC. We generated sample events for signal and background with `MadGraph5_aMC@NLO 2.6` [59], the showering and clustering were performed with `PYTHIA 8` [60], and finally, the detector simulation was done with `Delphes 3` [61]. For the SM background, we considered the Drell-Yan production of $Z/\gamma* \to \ell\ell$, with $\ell = e, \mu$, as in [50]. As in the toy model examples, we trained a `XGBoost` classifier, with 1M events per class, to distinguish S from B. We use as input parameters

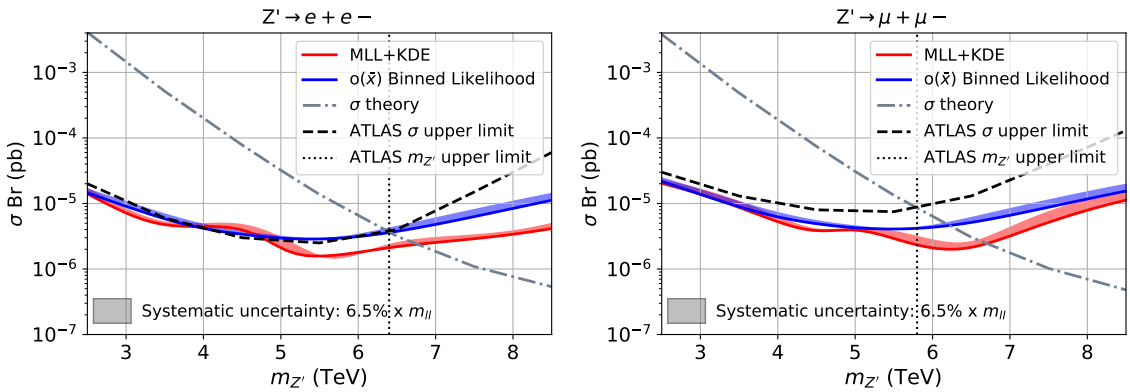

Figure 3: Exclusion limits for the Z'_{SSM} with MLL+KDE method (red curve), and with the BL fit of the ML output (blue curve). The shaded area in each case includes a naive estimation of the significance uncertainty caused by the mass variation on each point, according to the systematic uncertainty for the invariant mass estimated by ATLAS in [50]. *Left Panel:* Dielectron channel. *Right Panel:* Dimuon channel.

the transverse momentum $|p_T|$, the azimuthal angle ϕ, and the pseudorapidity η of the final state leptons in each channel, the kinematic variables that can be extracted directly from the `Delphes 3` output file.

We are employing the same setup and detector level cuts as in the work presented by the ATLAS Collaboration at $\sqrt{s} = 14$ TeV and 3 ab^{-1} [50], but we only generated signal and background events with dielectron and dimuon invariant masses above 1.8 TeV, and since we are dealing with a signal-enriched region and not the entire spectrum, the direct comparison with ATLAS projections for 95% CL exclusion limits is not strictly fair. This may enhance the performance of our classifier, since a Z' signal would appear as an excess at high dilepton invariant masses. However, the power of our method can be shown in the left (right) panel of Figure 3 for the dielectron (dimuon) channel when compared to the BL fit of the ML classifier output, which is on equal footing with the results for our method since it uses the same ML classifier. Unbinning signal and background posteriors provide more constraining exclusion limits for both final states.

4 Conclusions

The Machine-Learned Likelihoods method can be used to obtain discovery significances and exclusion limits for additive new physics scenarios. It uses a single classifier and its full one-dimensional output, which allows the estimation of the signal and background PDFs needed for statistical inference. In this paper, we extend the MLL method to obtain exclusion significances and improve its performance by using the KDE method to extract the corresponding PDFs from the ML output. Although the binning of the classifier output is always possible,

irrespective of the dimensionality of the original variables, we demonstrate that computing the PDFs with a non-parametric method such as KDE, avoiding the binning, enhances the performance. By analyzing toy models generated with Gaussian distribution of different dimensions, we showed that MLL with KDE outperforms the BL method when dealing with high-dimensional data, while for low-dimensional data all the methods converge to the results obtained with the true PDFs. Interestingly to note, MLL without binning improves also the exclusion-limits results obtained in a realistic Z' analysis, surpassing the ones computed with the simple BL fit of the ML one-dimensional output.

Acknowledgments. We thank Xabier Marcano, Manuel Szewc, and Alejandro Szynkman for fruitful discussions on the implementation of KDE in the MLL method. This work is partially supported by the "Atracción de Talento" program (Modalidad 1) of the Comunidad de Madrid (Spain) under the grant number 2019-T1/TIC-14019 (EA, RMSS), by the Spanish Research Agency (Agencia Estatal de Investigación) through the Grant IFT Centro de Excelencia Severo Ochoa No CEX2020-001007-S, funded by MCIN/AEI/10.13039/ 501100011033 (EA, MdlR, RMSS), and by CONICET and ANPCyT under projects PICT 2017-2751 and PICT 2018-03682 (EA, AP). MdlR also acknowledges financial support from the Comunidad Autónoma de Madrid through the grant SI2/PBG/2020-00005.

References

[1] A. J. Larkoski, I. Moult, and B. Nachman, *Jet Substructure at the Large Hadron Collider: A Review of Recent Advances in Theory and Machine Learning*, *Phys. Rept.* **841** (2020) 1–63, [arXiv:1709.04464].

[2] D. Guest, K. Cranmer, and D. Whiteson, *Deep Learning and its Application to LHC Physics*, *Ann. Rev. Nucl. Part. Sci.* **68** (2018) 161–181, [arXiv:1806.11484].

[3] K. Albertsson et al., *Machine Learning in High Energy Physics Community White Paper*, *J. Phys. Conf. Ser.* **1085** (2018), no. 2 022008, [arXiv:1807.02876].

[4] A. Radovic, M. Williams, D. Rousseau, M. Kagan, D. Bonacorsi, A. Himmel, A. Aurisano, K. Terao, and T. Wongjirad, *Machine learning at the energy and intensity frontiers of particle physics*, *Nature* **560** (2018), no. 7716 41–48.

[5] G. Carleo, I. Cirac, K. Cranmer, L. Daudet, M. Schuld, N. Tishby, L. Vogt-Maranto, and L. Zdeborová, *Machine learning and the physical sciences*, *Rev. Mod. Phys.* **91** (2019), no. 4 045002, [arXiv:1903.10563].

[6] D. Bourilkov, *Machine and Deep Learning Applications in Particle Physics*, *Int. J. Mod. Phys. A* **34** (2020), no. 35 1930019, [arXiv:1912.08245].

[7] G. Karagiorgi, G. Kasieczka, S. Kravitz, B. Nachman, and D. Shih, *Machine Learning in the Search for New Fundamental Physics*, arXiv:2112.03769.

[8] M. Feickert and B. Nachman, *A Living Review of Machine Learning for Particle Physics*, arXiv:2102.02770.

[9] T. Plehn, A. Butter, B. Dillon, and C. Krause, *Modern Machine Learning for LHC Physicists*, arXiv:2211.01421.

[10] B. H. Denby, *Neural Networks and Cellular Automata in Experimental High-energy Physics*, *Comput. Phys. Commun.* **49** (1988) 429–448.

[11] L. Lonnblad, C. Peterson, and T. Rognvaldsson, *Finding Gluon Jets With a Neural Trigger*, *Phys. Rev. Lett.* **65** (1990) 1321–1324.

[12] P. Baldi, P. Sadowski, and D. Whiteson, *Searching for Exotic Particles in High-Energy Physics with Deep Learning*, *Nature Commun.* **5** (2014) 4308, [arXiv:1402.4735].

[13] E. M. Metodiev, B. Nachman, and J. Thaler, *Classification without labels: Learning from mixed samples in high energy physics*, *JHEP* **10** (2017) 174, [arXiv:1708.02949].

[14] C. K. Khosa, V. Sanz, and M. Soughton, *Using machine learning to disentangle LHC signatures of Dark Matter candidates*, *SciPost Phys.* **10** (2021), no. 6 151, [arXiv:1910.06058].

[15] A. Mullin, S. Nicholls, H. Pacey, M. Parker, M. White, and S. Williams, *Does SUSY have friends? A new approach for LHC event analysis*, *JHEP* **02** (2021) 160, [arXiv:1912.10625].

[16] S. Chang, T.-K. Chen, and C.-W. Chiang, *Distinguishing W' signals at hadron colliders using neural networks*, *Phys. Rev. D* **103** (2021), no. 3 036016, [arXiv:2007.14586].

[17] F. Flesher, K. Fraser, C. Hutchison, B. Ostdiek, and M. D. Schwartz, *Parameter inference from event ensembles and the top-quark mass*, *JHEP* **09** (2021) 058, [arXiv:2011.04666].

[18] Y. S. Lai, D. Neill, M. Płoskoń, and F. Ringer, *Explainable machine learning of the underlying physics of high-energy particle collisions*, arXiv:2012.06582.

[19] B. Nachman and J. Thaler, *Learning from many collider events at once*, *Phys. Rev. D* **103** (2021), no. 11 116013, [arXiv:2101.07263].

[20] E. Arganda, A. D. Medina, A. D. Perez, and A. Szynkman, *Towards a method to anticipate dark matter signals with deep learning at the LHC*, *SciPost Phys.* **12** (2022) 063, [arXiv:2105.12018].

[21] K. Cranmer, J. Pavez, and G. Louppe, *Approximating Likelihood Ratios with Calibrated Discriminative Classifiers*, arXiv:1506.02169.

[22] A. Elwood and D. Krücker, *Direct optimisation of the discovery significance when training neural networks to search for new physics in particle colliders*, arXiv:1806.00322.

[23] R. T. D'Agnolo and A. Wulzer, *Learning New Physics from a Machine*, *Phys. Rev. D* **99** (2019), no. 1 015014, [arXiv:1806.02350].

[24] B. Nachman, *A guide for deploying Deep Learning in LHC searches: How to achieve*

optimality and account for uncertainty, *SciPost Phys.* **8** (2020) 090, [arXiv:1909.03081].

[25] R. T. D'Agnolo, G. Grosso, M. Pierini, A. Wulzer, and M. Zanetti, *Learning multivariate new physics*, *Eur. Phys. J. C* **81** (2021), no. 1 89, [arXiv:1912.12155].

[26] J. Hollingsworth and D. Whiteson, *Resonance Searches with Machine Learned Likelihood Ratios*, arXiv:2002.04699.

[27] K. T. Matchev, P. Shyamsundar, and J. Smolinsky, *A quantum algorithm for model independent searches for new physics*, arXiv:2003.02181.

[28] A. S. Cornell, W. Doorsamy, B. Fuks, G. Harmsen, and L. Mason, *Boosted decision trees in the era of new physics: a smuon analysis case study*, arXiv:2109.11815.

[29] J. A. Aguilar-Saavedra, *Anomaly detection from mass unspecific jet tagging*, *Eur. Phys. J. C* **82** (2022), no. 2 130, [arXiv:2111.02647].

[30] R. T. d'Agnolo, G. Grosso, M. Pierini, A. Wulzer, and M. Zanetti, *Learning New Physics from an Imperfect Machine*, arXiv:2111.13633.

[31] V. Mikuni, B. Nachman, and D. Shih, *Online-compatible unsupervised nonresonant anomaly detection*, *Phys. Rev. D* **105** (2022), no. 5 055006, [arXiv:2111.06417].

[32] C. K. Khosa, V. Sanz, and M. Soughton, *A simple guide from Machine Learning outputs to statistical criteria*, arXiv:2203.03669.

[33] M. Letizia, G. Losapio, M. Rando, G. Grosso, A. Wulzer, M. Pierini, M. Zanetti, and L. Rosasco, *Learning new physics efficiently with nonparametric methods*, arXiv:2204.02317.

[34] T. Finke, M. Krämer, M. Lipp, and A. Mück, *Boosting mono-jet searches with model-agnostic machine learning*, arXiv:2204.11889.

[35] F. F. Freitas, J. a. Gonçalves, A. P. Morais, and R. Pasechnik, *Phenomenology at the Large Hadron Collider with Deep Learning: the case of vector-like quarks decaying to light jets*, arXiv:2204.12542.

[36] E. Arganda, X. Marcano, V. M. Lozano, A. D. Medina, A. D. Perez, M. Szewc, and A. Szynkman, *A method for approximating optimal statistical significances with machine-learned likelihoods*, *Eur. Phys. J. C* **82** (2022), no. 11 993, [arXiv:2205.05952].

[37] **ATLAS** Collaboration, G. Aad et al., *Measurement of the t-channel single top-quark production cross section in pp collisions at $\sqrt{s} = 7$ TeV with the ATLAS detector*, *Phys. Lett. B* **717** (2012) 330–350, [arXiv:1205.3130].

[38] **ATLAS** Collaboration, G. Aad et al., *Search for the electroweak production of supersymmetric particles in $\sqrt{s}$=8 TeV pp collisions with the ATLAS detector*, *Phys. Rev. D* **93** (2016), no. 5 052002, [arXiv:1509.07152].

[39] **CMS** Collaboration, A. M. Sirunyan et al., *Search for new phenomena in final states with two opposite-charge, same-flavor leptons, jets, and missing transverse momentum in pp collisions at $\sqrt{s} = 13$ TeV*, *JHEP* **03** (2018) 076, [arXiv:1709.08908].

[40] **CMS** Collaboration, A. M. Sirunyan et al., *Evidence for associated production of a Higgs boson with a top quark pair in final states with electrons, muons, and hadronically decaying τ leptons at $\sqrt{s} = 13$ TeV*, *JHEP* **08** (2018) 066, [arXiv:1803.05485].

[41] **CMS** Collaboration, A. M. Sirunyan et al., *Measurement of the production cross section for single top quarks in association with W bosons in proton-proton collisions at $\sqrt{s} = 13$ TeV*, *JHEP* **10** (2018) 117, [arXiv:1805.07399].

[42] **CMS** Collaboration, A. M. Sirunyan et al., *Search for supersymmetry in final states with two oppositely charged same-flavor leptons and missing transverse momentum in proton-proton collisions at $\sqrt{s} = 13$ TeV*, *JHEP* **04** (2021) 123, [arXiv:2012.08600].

[43] **ATLAS** Collaboration, G. Aad et al., *Measurement of the $t\bar{t}t\bar{t}$ production cross section in pp collisions at $\sqrt{s} = 13$ TeV with the ATLAS detector*, *JHEP* **11** (2021) 118, [arXiv:2106.11683].

[44] **ATLAS** Collaboration, *Measurements of Higgs boson production by gluon−gluon fusion and vector-boson fusion using $H \to WW^* \to e\nu\mu\nu$ decays in pp collisions at $\sqrt{s} = 13$ TeV with the ATLAS detector*, arXiv:2207.00338.

[45] "A method for approximating optimal statistical significances with machine-learned likelihoods." https://github.com/AndresDanielPerez/2205.05952-ML-Likelihood-method, 2021.

[46] E. Arganda, M. de los Rios, A. D. Perez, and R. M. Sandá Seoane, *Imposing exclusion limits on new physics with machine-learned likelihoods*, *PoS* **ICHEP2022** (2022) 1226.

[47] M. Rosenblatt, *Remarks on Some Nonparametric Estimates of a Density Function*, *Ann. Math. Statist.* **27** (1956), no. 3 832–837.

[48] E. Parzen, *On Estimation of a Probability Density Function and Mode*, *Ann. Math. Statist.* **33** (1962), no. 3 1065–1076.

[49] G. Altarelli, B. Mele, and M. Ruiz-Altaba, *Searching for New Heavy Vector Bosons in $p\bar{p}$ Colliders*, *Z. Phys. C* **45** (1989) 109. [Erratum: Z.Phys.C 47, 676 (1990)].

[50] **ATLAS** Collaboration, G. Aad et al., *Prospects for searches for heavy Z' and W' bosons in fermionic final states with the ATLAS experiment at the HL-LHC*, *ATL-PHYS-PUB-2018-044* (2018).

[51] K. Cranmer et al., *Publishing statistical models: Getting the most out of particle physics experiments*, *SciPost Phys.* **12** (2022) 037, [arXiv:2109.04981].

[52] G. Cowan, K. Cranmer, E. Gross, and O. Vitells, *Asymptotic formulae for likelihood-based tests of new physics*, *Eur. Phys. J. C* **71** (2011) 1554, [arXiv:1007.1727]. [Erratum: Eur.Phys.J.C 73, 2501 (2013)].

[53] J. Neyman and E. S. Pearson, *On the Problem of the Most Efficient Tests of Statistical Hypotheses*, *Phil. Trans. Roy. Soc. Lond. A* **231** (1933), no. 694-706 289–337.

[54] G. J. McLachlan and K. E. Basford, *Mixture models : inference and applications to clustering*, 1988.

[55] G. Papamakarios, *Neural Density Estimation and Likelihood-free Inference*. PhD thesis, Edinburgh U., 4, 2019. arXiv:1910.13233.

[56] R. Gomez Ambrosio, J. ter Hoeve, M. Madigan, J. Rojo, and V. Sanz, *Unbinned multivariate observables for global SMEFT analyses from machine learning*, arXiv:2211.02058.

[57] F. Pedregosa, G. Varoquaux, A. Gramfort, V. Michel, B. Thirion, O. Grisel, M. Blondel, P. Prettenhofer, R. Weiss, V. Dubourg, J. Vanderplas, A. Passos, D. Cournapeau, M. Brucher, M. Perrot, and E. Duchesnay, *Scikit-learn: Machine learning in Python*, *Journal of Machine Learning Research* **12** (2011) 2825–2830.

[58] V. A. Epanechnikov, *Non-parametric estimation of a multivariate probability density*, *Theory of Probability and its Applications* **14** (1969), no. 1 153–158.

[59] J. Alwall, R. Frederix, S. Frixione, V. Hirschi, F. Maltoni, O. Mattelaer, H. S. Shao, T. Stelzer, P. Torrielli, and M. Zaro, *The automated computation of tree-level and next-to-leading order differential cross sections, and their matching to parton shower simulations*, *JHEP* **07** (2014) 079, [arXiv:1405.0301].

[60] T. Sjöstrand, S. Ask, J. R. Christiansen, R. Corke, N. Desai, P. Ilten, S. Mrenna, S. Prestel, C. O. Rasmussen, and P. Z. Skands, *An Introduction to PYTHIA 8.2*, *Comput. Phys. Commun.* **191** (2015) 159–177, [arXiv:1410.3012].

[61] **DELPHES 3** Collaboration, J. de Favereau, C. Delaere, P. Demin, A. Giammanco, V. Lemaître, A. Mertens, and M. Selvaggi, *DELPHES 3, A modular framework for fast simulation of a generic collider experiment*, *JHEP* **02** (2014) 057, [arXiv:1307.6346].